Journal of Integrative Neuroscience

J. Integr. Neurosci. **2025**; 24(3): 25710
https://doi.org/10.31083/JIN25710

Original Research

FKBP51 is Involved in Epileptic Seizure by Regulating PSD95 in a PTZ-Induced Epileptic Mouse Model

Ling Chen[1,†], Wenxiu Cui[1,2,†], Jiyao Qin[1], Manmin Zhu[1], Haiqing Zhang[1], Juan Yang[1], Zucai Xu[1], Hao Huang[1,*]

[1]Department of Neurology, Affiliated Hospital of Zunyi Medical University, 563000 Zunyi, Guizhou, China
[2]Department of Neurology, Ziyang Central Hospital, 641300 Ziyang, Sichuan, China
*Correspondence: haohuang325@163.com (Hao Huang)
[†]These authors contributed equally.
Academic Editor: Bettina Platt
Submitted: 15 July 2024 Revised: 10 December 2024 Accepted: 20 December 2024 Published: 19 March 2025

Abstract

Background: Epilepsy, the world's third most prevalent chronic brain disorder, significantly affects patients' quality of life and increases the economic burden on families and society. Previous studies have demonstrated that FK506-binding protein 51 (FKBP51) plays a crucial role in synaptic plasticity. However, FKBP51 exhibits different functions under various physiological and pathological conditions. Our study explored the relationship between FKBP51 and epilepsy and its possible mechanism of action. We also analyzed the expression levels of postsynaptic density-95 (PSD95) and synaptophysin (SYP) in the hippocampus to examine the pathophysiology of epilepsy. **Methods**: A chronic epileptic kindling model was established by injecting pentylenetetrazole (PTZ) intraperitoneally, and a spontaneous seizure model was created by injecting kainic acid (KA) into the dentate gyrus using a stereotaxic apparatus. Endogenous FKBP51 expression was inhibited using adeno-associated virus (AAV)-FKBP51-Small hairpin RNAs (shRNA). The expression of FKBP51, PSD95, and SYP in the hippocampus and synaptosomes was measured through western blotting. Golgi staining and electron microscopy were used to examine spines and synaptic structures. **Results**: The results showed a significant increase in FKBP51 expression in the hippocampal tissue of the PTZ- and KA-induced epilepsy model groups. Inhibition of FKBP51 expression through AAV-FKBP51-shRNA resulted in a shorter latency and an elevated seizure grade score in mice. Moreover, the suppression of FKBP51 expression enhanced the expression of synaptic plasticity-related proteins, increased the density of dendritic spines, and elevated the quantity of spherical synaptic vesicles in the presynaptic membrane in the hippocampus. **Conclusions**: FKBP51 may serve as an endogenous protective factor in epilepsy by regulating the expression of the synaptic plasticity-related protein PSD95, the density of dendritic spines, and the number of synaptic vesicles in the hippocampal CA1.

Keywords: FK506 binding protein 51; epilepsy; postsynaptic density protein 95; synaptic plasticity; dendritic spine

1. Introduction

Epilepsy is the third most common chronic brain disorder worldwide [1]. Presently, there are approximately 70 million patients with epilepsy worldwide, with 9 million in China, having an annual increase rate of 400,000 to 500,000 cases [2]. Although existing antiseizure medications targeting neurons and synapses have achieved certain clinical efficacy, 20–30% of patients with epilepsy still develop drug-resistant epilepsy (refractory epilepsy) [3,4]. As a chronic disease characterized by repeated seizures, epilepsy significantly affects patients' quality of life and increases the economic burden on families and society. It has emerged as a public health problem recognized by society [5,6]. However, the specific pathogenesis of epilepsy remains unknown. Therefore, identifying the mechanisms underlying epilepsy is paramount for identifying effective therapeutic strategies.

Abnormal synaptic connections between neurons gradually enhance neuronal excitability, increasing susceptibility to spontaneous seizures in epilepsy [7,8]. A synapse is a structure formed by interneuronal connections specialized for point-to-point information transfer from a presynaptic neuron to a postsynaptic cell [9,10]. Furthermore, synaptic transmission is influenced by the presynaptic exocytosis of synaptic vesicles containing neurotransmitters and the reaction of these neurotransmitters with postsynaptic receptors [9]. A previous study revealed the essential roles of axons, dendrites, and synaptic connections in neurotransmission, neural circuits, synaptic plasticity, and other neuronal physiology [11]. Through this communication structure, nerve cells form functional neural circuits for transmitting and storing information. Synapses can undergo specific structural changes under the influence of continuous neuronal activity, known as "synaptic structural plasticity" [6]. Synaptic plasticity is the neurons' ability to modify their connections, mainly manifested through changes in dendritic spine morphology and number, synaptic morphology and density, and the formation of new synapses [12,13]. Neuronal dendrite and dendritic spine formation are essential for normal synaptic transmis-

sion. A study has demonstrated that the remodeling of neuronal synaptic structures is involved in epilepsy occurrence [14].

FK506-binding protein 51 (FKBP51), highly expressed and involved in physiological processes in the central nervous system (CNS), plays a novel role in neuronal synaptic plasticity [15,16]. The gene encoding FKBP51, FKBP5, is located at 6p21.31 in humans and consists of 13 exons and 12 introns across over 150 kb of genomic DNA [17]. FKBP51 is found in fat cells, skeletal muscles, and various brain regions [18]. FKBP51 is mainly expressed in the cortex and hippocampus in rodent brains. It is primarily involved in regulating pathways related to immune function, autophagy, epigenetic remodeling, apoptosis, cell growth, cytoskeletal dynamics, and metabolism. Additionally, it is associated with various neurological diseases, including Parkinson's disease, Alzheimer's disease, post-traumatic stress disorder, schizophrenia, and depression [15,19,20]. FKBP51 is crucial in synaptic plasticity [21] and is primarily localized in excitatory neurons within the neocortex [22]. FKBP51 expression is negatively correlated with dendritic spines and strongly negatively correlated with mushroom dendritic spines in the superficial layer neurons of the neocortex of schizophrenic patients [22]. Inhibiting FKBP51 expression promotes axon and dendrite growth on neurons and regulates microtubule-related protein expression, potentially increasing neuronal excitability. Conversely, the overexpression of FKBP51 may inhibit axon length and dendritic growth through the upregulation of RhoA activity, thereby decreasing neuronal excitability [23,24]. A previous study found that SAFit2 (a specific inhibitor of FKBP51) could promote axonal growth and enhance neurite growth and the number of branch points in primary hippocampal neuron cultures [25]. Additionally, SAFit2 increases hippocampal neural progenitor cell neurogenesis and the axonal complexity and length of these differentiated neurons [25]. In contrast, Qiu *et al*. [26] found that long-term potentiation (LTP) is reduced in FKPB51 knockout (KO) mice, leading to decreased neuronal excitability and alterations in glutamatergic and γ-aminobutyric acid (GABA)ergic signaling pathways. The frequency of miniature excitatory postsynaptic currents (mEPSCs) was decreased in the hippocampus of KO mice, indicating a reduction in excitatory synaptic activity. Therefore, the current findings regarding FKBP51 are incongruous. To address this, we utilized adeno-associated virus (AAV) transfection to reduce FKBP51 expression and investigate its involvement in the onset of epilepsy and the potential underlying mechanisms.

Postsynaptic density-95 (PSD95) is an abundant postsynaptic protein in excitatory synapses that plays an important role in regulating synaptic strength and synaptic plasticity processes [27,28]. Bayés *et al*. [29] have highlighted the importance of the PSD95 protein in epilepsy research. Studies indicate that PSD95 can modulate synaptic transmission by influencing the function of N-methyl-D-aspartic acid (NMDA) and α-amino-3-hydroxy-5-methyl-4-isoxazole-propionic acid (AMPA) receptors [30–32]. In a mouse model of cyclin-dependent kinase-like 5 (CDKL5) deficiency epilepsy, the abnormal activation of the brain-derived neurotrophic factor-tropomyosine receptor kinase B (BDNF-TrkB) signaling pathway led to enhanced excitatory synaptic transmission and epileptic seizures, which may be associated with reduced expression of PSD95 [33]. Synaptophysin (SYP) is a specific calcium-binding protein with a relative molecular weight of 38 kDa and is predominantly located on the synaptic vesicle membrane of neurons [10]. SYP is a structural glycoprotein that regulates neurotransmitter release and the development and growth of neuronal protrusions [34]. Upregulation of SYP has been reported to have antiepileptic effects and cognitive benefits, in addition to enhancing synaptic plasticity in the hippocampus [35]. Moreover, SYP has the potential to serve as a biomarker for synaptic transmission and reconstruction [36]. Studies have found that SYP is important in synaptic vesicle fusion with the presynaptic membrane, making it essential for neurotransmitter release, which provides insights into the density, distribution, number, and efficiency of synaptic transmission [37–39]. Consequently, we analyzed the expression levels of PSD95 and SYP in synaptosomes in the hippocampus of control and epileptic mice to examine the pathophysiology of epilepsy.

The role of FKBP51 in epilepsy may be quite complex, potentially serving different functions under various physiological and pathological conditions. In some instances, FKBP51 may regulate neuronal excitability, while in others, it may contribute to suppressing excessive neuronal activity. Our goal for this study was, therefore, to explore the relationship between FKBP51 and PTZ- and kainic acid (KA)-induced epilepsy, investigate its possible mechanisms, and examine the pathophysiology of epilepsy by analyzing the expression of PSD95 and SYP in the hippocampus of control and epileptic mice.

2. Materials and Methods

2.1 Animals

This study selected healthy male C57BL/6 mice aged 7–8 weeks and weighing approximately 25–30 g as the research subjects. They were kept in separate cages under a constant temperature of 23 $\pm$ 2 °C with a 12-h alternating day and night cycle, during which they had free access to food and water. All C57BL/6 mice were purchased from Spiff (Beijing, China) Biotechnology Co., Ltd. (License: SCXK (Beijing, China) 2019-0010) and housed at the Medical Laboratory Animal Center of our university. All animal experiments adhered to the Guide for the Care and Use of Laboratory Animals (NIH Publication No. 80-23) and were approved by the Ethics Committee of Affiliated Hospital of Zunyi Medical University, with Ethics Review Batch Number: KLLY (A)-2021-02.

2.2 Establishment of Animal Model

2.2.1 Pentylenetetrazole-Induced Chronic Kindling Model of Mice

Pentylenetetrazole (PTZ, P6500, Merck & Co., Inc., Rahway, NJ, USA) was dissolved in 0.9% sterile normal saline at a concentration of 2 mg/mL for immediate use. The weight of each mouse was measured before each injection, and the corresponding dose of PTZ was administered intraperitoneally based on the individual mouse's weight. PTZ was injected into the lower left or lower right quadrant of the animal's abdomen. PTZ (35 mg/kg) and the same volume of saline were intraperitoneally injected into mice in the Model group and Control (Con) group, respectively, every other day for 30 days (15 times in total), and their behavior was observed for 30 min after each PTZ injection [40,41]. The severity of seizures was scored, and the incubation period was recorded. Three consecutive seizures of grade 3 and above were considered a successful induction of the PTZ chronic epilepsy model.

The seizure behavior of the mice in each group was mainly recorded regarding seizure grade and latency. The seizure latency period was defined as the time from the first intraperitoneal injection of PTZ to the complete induction of the chronic epileptic model.

Seizure grading [41]: Grade 0: absence of response and abnormalities; Grade 1: immobilization in a prone position; Grade 2: head nodding, twitching of the ears and face, myoclonic movements in forelimbs or hindlimbs; Grade 3: persistent whole-body myoclonus, myoclonic spasms, tail rigidly upright; Grade 4: collapse to one side, erratic running and jumping, tonic convulsions; Grade 5: generalized tonic-clonic seizures; Grade 6: lethal outcome.

2.2.2 KA-Induced Epilepsy Model of Mice

An intraperitoneal injection of pentobarbital sodium (0.3%, 50 mg/kg, P3761, Sigma-Aldrich, St. Louis, MO, USA) was administered to the mice, which were deeply anesthetized and fixed in a stereotaxic apparatus (68025, RWD, Guangdong, China). The skin on the top of the head was trimmed. Subsequently, the surgical area on the mouse's head was thoroughly disinfected with iodophor, and the scalp was cut along the midline to fully expose the surgical area and bregma points. KA (anteroposterior (AP): 1.6 mm; mediolateral (ML): 1.5 mm; dorsoventral (DV): 2.0 mm, K911410, MACKLIN, Shanghai, China) was injected into the dentate gyrus of the hippocampus. After positioning, an electric micro-animal skull drill (SD-300, Shanghai Yuyan Scientific Instrument Co., Ltd, Shanghai, China) was used to open the skull. Subsequently, a 2-μL micro-syringe (KDS LEGATO 130, RWD, Guangdong, China) was employed to absorb 1.0 nmol of KA solution (50 nL); the needle was slowly inserted vertically at the drilling site, and the solution was injected at a rate of 5 nL/min. After each injection, the needle was gently removed after being left in place for 10 min to prevent regurgitation. The anchor point was sealed with dental cement; no active bleeding was observed, and the scalp was sterilized layer by layer. The mice were disinfected, labeled, and placed in a warm environment until they awoke. Mouse behavior was observed via video detection for 30 days, with spontaneous seizures considered successful models. The behavioral score was similar to that of the PTZ-induced chronic kindling epileptic mouse model.

2.3 Construction and Stereotaxic Injection of AAV-FKBP51-shRNA for Hippocampal CA1 and CA3

The expression of endogenous FKBP51 in hippocampal neurons was lowered by applying AAV-FKBP51-shRNA. Syngentech Company, located in Beijing, China, developed and synthesized three AAV-FKBP51-shRNA sequences (shRNA1: 5′-AGAAAGACAGAGGAGTATTAA-3′; shRNA2: 5′-AGGCGAGATCTGCCATTTATT-3′; shRNA3: 5′-ATTTCAAAGGTGAGGATTTAT-3′; Backbone in (**Supplementary Fig. 1**) (The certificate of analysis of the primers is given in **Supplementary Material-1**.). To determine whether FKBP51 is expressed in the hippocampus of mice, western blotting was utilized to select the most effective AAV-FKBP51-shRNA gene sequence. AAV-GFP served as the vehicle for AAV-FKBP51-shRNA. Mice were anesthetized with pentobarbital sodium (0.3%, 50 mg/kg, P3761, Sigma-Aldrich, St. Louis, MO, USA). Then, a stereotaxic apparatus (68025, RWD, Guangdong, China) was used to inject saline and three AAV-FKBP51-shRNA sequences into the mice's hippocampus. Bilateral multi-point injections (AP: –2 mm; ML: 1.5 mm; DV: 1.5 mm; and AP: –2 mm; ML: 2.5 mm, DV: 1.3 mm) were performed relative to the bregma point to increase transfection efficiency. First, after the corresponding coordinates were marked, the skull was drilled using an electric micro-animal skull drill. Subsequently, 2-μL AAV-GFP and AAV-FKBP51-shRNA was drawn with a micro-syringe; the needle was slowly inserted vertically into the drilling site, and the solution was injected at a rate of 0.1 μL/min. The needle was held in place for 10 min after each injection to prevent regurgitation of the infusion. The anchor point was then sealed with dental cement. No active bleeding was observed. The mice were disinfected, labeled, and placed in a warm environment until they regained consciousness.

2.4 Cardiac Perfusion Slicing

Four weeks after AAV transfection, mice were anesthetized with an intraperitoneal injection of 0.3% pentobarbital sodium (50 mg/kg, P3761, Sigma-Aldrich, St. Louis, MO, USA). They were placed supine on the operating table, and their limbs were secured with rubber bands. The skin under the xiphoid process of the mice was pulled with tweezers, and the skin, subcutaneous tissue, and peritoneum were cut layer by layer. The chest was opened to fully

expose the heart, which was held with tweezers using the left hand. The puncture needle was slowly inserted at the heart's apex with the right hand, the front part was fixed using hemostatic forceps, and the right auricle was quickly cut off. The liver was slowly injected with phosphate-buffered saline (PBS) until it turned white, which was then fixed by a rapid infusion of 4% paraformaldehyde (P804536, MACKLIN, Shanghai, China). Once the mouse's tail and limbs stiffened, the brain was carefully removed from the cranium, and the tissues were fixed in 4% paraformaldehyde for 24 h. For the frozen section, the brain tissue was transferred to a 30% sucrose solution (S769550, MACKLIN, Shanghai, China), allowed to settle, and subsequently removed. Parts of the forehead and cerebellar tissues were trimmed using a blade. After embedding was complete, the tissues were placed in a –80 °C refrigerator (DW-86L388A, Haier, Qingdao, China) for 30 min, and coronal sections were performed using a frozen microtome (CM1950, Leica, Wetzlar, Germany). AAVs exhibited green fluorescence and were observed using a fluorescence microscope (IXplore Standard, Olympus Corporation, Tokyo, Japan) immediately after removal, and images were captured.

2.5 Western Blotting

The mice's hippocampal tissues were taken out of a –80 °C refrigerator (DW-86L388A, Haier, Qingdao, China) and weighed, placed on ice, and added with corresponding doses of radioimmunoprecipitation assay buffer (RIPA, R0010, Solarbio Science & Technology Co., Ltd., Beijing, China) and phenylmethylsulfonyl fluoride (PMSF, P0100, Solarbio Science & Technology Co., Ltd., Beijing, China). Subsequently, the hippocampal tissues were homogenized and centrifuged using an ultrasonic crusher. A bicinchoninic acid (BCA) quantitative kit (PC0020, Solarbio Science & Technology Co., Ltd., Beijing, China) was used for quantification. Based on molecular weight, a sodium dodecyl sulfate-polyacrylamide gel electrophoresis (SDS-PAGE) was selected, and the protein samples (10 µL) were separated. At a constant current of 250 mA, the appropriate time was determined based on the molecular weight of the target protein. The membranes were subsequently rinsed with Tris-buffered saline (T1010, Solarbio Science & Technology Co., Ltd., Beijing, China) and 0.1% Tween® 20 detergent (TBST, P1001, Solarbio Science & Technology Co., Ltd., Beijing, China) on a shaker for 5 min and blocked with 5% skim milk powder for 2 h. This was followed by washing with TBST for 5 min thrice. FKBP51 rabbit antibodies (1:1000, 14155-1-AP, Proteintech Group, Inc, Wuhan, China), PSD95 rabbit antibodies (1:5000, 20665-1-AP, Proteintech Group, Inc, Wuhan, China), SYP rabbit antibodies (1:40,000, Cat No. 17785-1-AP, Proteintech Group, Inc., Wuhan, China), GAPDH rabbit antibodies (1:10,000, 10494-1-AP, Proteintech Group, Inc, Wuhan, China), and β-tubulin mouse antibodies (1:50,000, 66240-1-Ig, Proteintech Group, Inc, Wuhan, China) were added and incubated overnight on a shaking table at 4 °C. Secondary antibodies (rabbit secondary antibodies [1:10,000, SA00001-2, Proteintech Group, Inc, Wuhan, China] or mouse secondary antibodies [1:50,000, SA00001-1, Proteintech Group, Inc, Wuhan, China]) were prepared. A polyvinylidene fluoride membrane was placed in a diluent of secondary antibodies prepared with 5% skim milk and incubated at room temperature for 1 h. The parameters were adjusted, and exposure was created.

2.6 Immunofluorescence Staining

The prepared paraffin specimens were placed in xylene I and II (X821391, MACKLIN, Shanghai, China) for 20 min each and dewaxed using an alcohol gradient. Antigen repair was performed with 0.01 M sodium citrate buffer (C1010, Solarbio Science & Technology Co., Ltd., Beijing, China), and 0.3% TritonX-100 (IT9100, Solarbio Science & Technology Co., Ltd., Beijing, China) drops were added to the section for membrane breakage. Subsequently, ready-to-use goat serum was dropped onto the brain tissue, and the specimens were incubated at 37.0 °C for 40 min. FKBP51 antibody (PBS dilution ratio 1:50, P787575, MACKLIN, Shanghai, China) and NeuN antibody (PBS dilution ratio 1:200, 26975-1-AP, Proteintech Group, Inc, Wuhan, China) or glial fibrillary acidic protein (GFAP) antibody (PBS dilution ratio 1:200, CL488-16825, Proteintech Group, Inc, Wuhan, China) were evenly mixed and added to the slices, which were then stored in a refrigerator at 4 °C for at least 15 h. The following day, they were reheated for 45 min. The slices were incubated with 488-labeled anti-rat fluorescent secondary antibody (1:200, RGAM002, Proteintech Group, Inc, Wuhan, China) and 594-labeled anti-rabbit fluorescent secondary antibody (1:500, HA1122, HuaAn Biotechnology Co., Ltd, Zhejiang, China) in a wet box at 37 °C for 80 min. The slices were sealed with an anti-fluorescence attenuator containing 4′,6-diamidino-2-phenylindole (DAPI, S2110, Solarbio Science & Technology Co., Ltd., Beijing, China), and a fluorescence microscope (IXplore Standard, Olympus Corporation, Tokyo, Japan) was used to observe and capture the images.

2.7 Synaptic Vesicle Extraction

The required amount of Syn-PER reagent (87793, Thermo Fisher Scientific Inc., Waltham, MA, USA) was calculated according to the sample size, and protease (P6730, Solarbio Science & Technology Co., Ltd., Beijing, China) and phosphatase inhibitors (P1206, Solarbio Science & Technology Co., Ltd., Beijing, China) were used to reduce the final inhibitor concentration to 1×. The mass of hippocampal tissue was measured and added to the aforementioned mixture at a rate of 10 µL/mg. The hippocampal tissue was homogenized on ice using an ultrasonic crusher (LD-CP650, Shandong Lande Intelligent Technology Co., Ltd., Liaocheng, Shangdong, China). The tube was subse-

quently centrifuged (4 °C, 1200 ×g, 10 min). After centrifugation, the supernatant was transferred to a clean Eppendorf tube. The tube was centrifuged again (4 °C, 15,000 ×g, 20 min), the supernatant was discarded, and the precipitate was retained. Syn-PER reagent was added to the precipitate at 1 µL/mg for resuspension, and the mixture was stored at –80 °C for later use. The remaining steps were similar to those used for western blotting. All steps, including homogenization and centrifugation, were performed at 4 °C to reduce proteolysis, dephosphorylation, and denaturation.

2.8 Golgi Staining

Golgi-Cox staining was performed using an FD Rapid GolgiStain Kit (PK401, FD Neuro Technologies, Ellicott City, MD, USA. One day in advance, a solution A and B mixture was prepared in a 1:1 ratio, incubated at room temperature away from light, and the supernatant was collected 24 h later. The mice were deeply anesthetized after injection of 0.3% pentobarbital sodium (50 mg/kg, P3761, Sigma-Aldrich, St. Louis, MO, USA); the brain was quickly extracted, and the blood on the brain tissue's surface was washed off with double-distilled water. The brain tissue was cut into small pieces of approximately 1 cm thickness using a blade. These tissue pieces were completely immersed in the AB mixture and incubated in the dark at room temperature for 24 h, followed by replacement of the AB solution with fresh solution. After soaking in the dark at room temperature for 2 weeks, the brain tissue was transferred to a certain amount of solution C (5 mL/cm^3), which was subsequently replaced after incubation in the dark at room temperature for 24 h, 2 days, and 3 days. The soaked brain tissue was removed from solution C, and the microtome's thickness was adjusted to 100 µm for continuous coronal sections, followed by Golgi staining. The sections were placed in a mixture of equal parts of solutions D and E and double-distilled water (1:1:2 ratio) for Golgi staining for 10 min, followed by rinsing with double-distilled water twice for 4 min each. The quantitative analysis of dendritic spine density was performed using the Skeletonize tool in ImageJ software (version 1.8.0, National Institute of Health, Bethesda, MD, USA).

2.9 Transmission Electron Microscopy

Samples from the CA1 region of the fresh hippocampal tissue were cut into small pieces of ~1 mm after fixation. The samples were first fixed in 2.5% glutaraldehyde (P1126, Solarbio Science & Technology Co., Ltd., Beijing, China) at 4 °C for 3 h and then in 1% osmic acid (CB0853316, ChemicalBook, Beijing, China) at 4 °C for 2 h. Subsequently, gradient dehydration, infiltration embedding, and resin polymerization were performed. Ultrathin sections with a thickness of 70 nm were made using an ultrathin microtome (UC ENUITY, Leica, Wetzlar, Germany). The slices were picked up with a copper mesh, stained with lead citrate solution (L885990, MACKLIN, Shanghai, China) and observed and photographed using a transmission electron microscope (JEOL JEM-F200, JEOL Japan Electronics Co., Ltd, Tokyo, Japan). We used ImageJ (version 1.8.0, National Institute of Health, Bethesda, MD, USA), an image analysis software, for processing to quantitatively analyze the density of neuronal dendritic spines.

2.10 Statistical Analysis

In this study, data analysis and statistics were conducted using SPSS (version 29.0.2.0, IBM SPSS statistics, Chicago, IL, USA) and ImageJ software (version 1.8.0, National Institute of Health, Bethesda, MD, USA). Statistical charts were created using GraphPad Prism software (version 9.4.0.673, GraphPad Software Inc., San Diego, CA, USA). Experimental data are expressed as mean ± standard deviation ($\bar{x} \pm$ s). Student's *t*-test was utilized for comparisons between two groups, and $p < 0.05$ was considered statistically significant. The one-way analysis of variance (ANOVA) was employed for comparisons between three groups. The Bonferroni post-hoc test was typically used for multiple comparisons following one-way ANOVA to determine whether significant differences exist between the three or more groups. We set $\alpha < 0.05/n$ (n = the number of comparisons between groups) as the level of significance for the test. For comparison among the three groups, the adjusted $\alpha' = 0.05/3$, $\alpha' < 0.0167$ was considered statistically significant, and the comparison among the four groups, $\alpha' = 0.05/6$, $\alpha' < 0.0083$ was considered statistically significant.

3. Results

3.1 Expression of FKBP51, PSD95, and SYP Proteins in the Hippocampus of Mice in Normal and Epileptic Model Groups

Western blotting was used to evaluate FKBP51, PSD95, and SYP expression in the hippocampal tissues of normal and epileptic model mice. The results revealed that compared to the Con group, there was a significant upregulation of FKBP51 expression in the hippocampal tissues of PTZ and KA model mice ($p < 0.01$). Due to the requirement of stereotactic techniques for the KA-induced epilepsy model, to avoid potential interactions between drugs during the later stages of stereotactic injection of adeno-associated viruses, the PTZ-induced chronic kindling model was selected for further experiments. The overall protein expression levels of PSD95 and SYP did not differ significantly between the Con and Model groups ($p > 0.05$). Thus, we investigated the expression of PSD95 and SYP in hippocampal synaptosomes. The results demonstrated that compared to the Con group, the hippocampal synaptosomes in the Model group exhibited reduced expression of PSD95 and SYP proteins, with statistically significant differences ($p < 0.01$) (n = 5, Fig. 1 and the original figures of western blot can be found in the **Supplementary Fig. 2**).

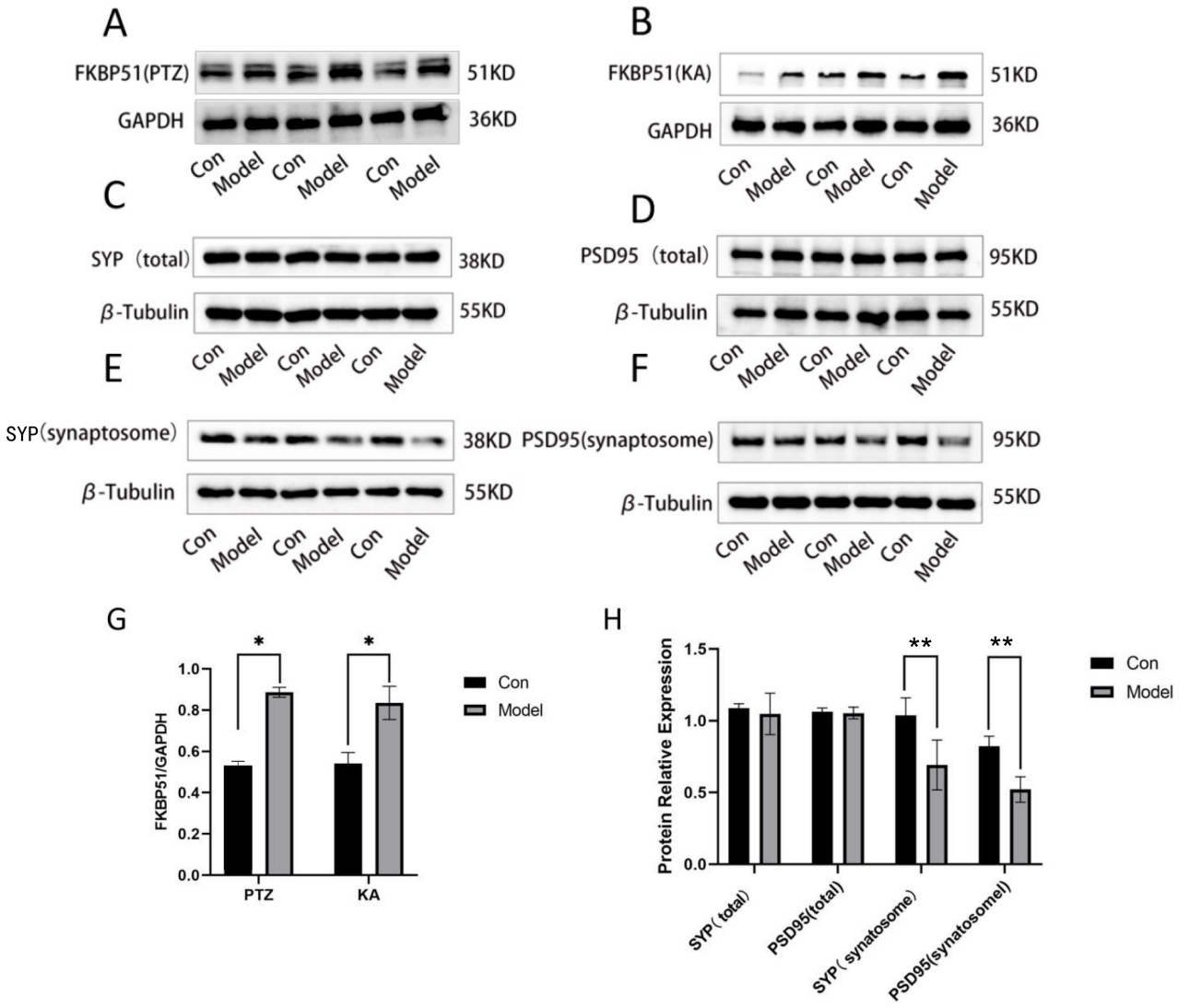

Fig. 1. Expression of FKBP51 and SYP in PTZ and KA epileptic mouse models. (A,B) Expression of FKBP51 in PTZ and KA epileptic mouse models. (C–F) Expression of "total SYP and PSD95" and "SYP and PSD95 after extraction of synaptosomes" in the hippocampus of normal and epileptic mice in the PTZ epileptic mouse model. (G) Quantitative analysis of FKBP51 expression between the Con group and Model group in PTZ and KA epileptic models. (n = 5, Student's t-test: T = 21.663, $*p = 0.0039 < 0.01$, vs. Con group). (H) Bar chart of PSD95 and SYP expression in the PTZ model (n = 5, Student's *t*-test: T = 21.663, $**p = 0.0039 < 0.01$, vs. Con group). FKBP51, FK506-binding protein 51; SYP, synaptophysin; PTZ, pentylenetetrazole; KA, kainic acid; PSD95, postsynaptic density-95.

3.2 Localization of FKBP51 in Epileptic Brain Tissue by Immunofluorescence Detection

Immunofluorescence was used to determine the localization of FKBP51 in the hippocampus of epileptic mice. The results revealed that FKBP51 was expressed in the CA1 of the hippocampus of epileptic mice, while it was co-expressed with NeuN, a neuron-specific marker, and with glial fibrillary acidic protein (GFAP), a specific astrocyte marker (n = 5, Fig. 2).

3.3 Detection of AAV Transfection Rate

Four weeks after bilateral stereoscopic injection of AAV-FKBP51-shRNA in the hippocampal CA1, immunofluorescence revealed the expression of fluorescent proteins in the hippocampal CA1 and CA3 (Fig. 3A–C). Western blotting was used to detect the expression of FKBP51 protein in the hippocampus after inhibition of each sequence. The results indicated that the expression of FKBP51 protein decreased in the transfection group compared to the PTZ+AAV-GFP group. The AAV-FKBP51-shRNA1 sequence inhibited approximately 7.3% expression of FKBP51 protein ($\alpha' > 0.0083$), while the

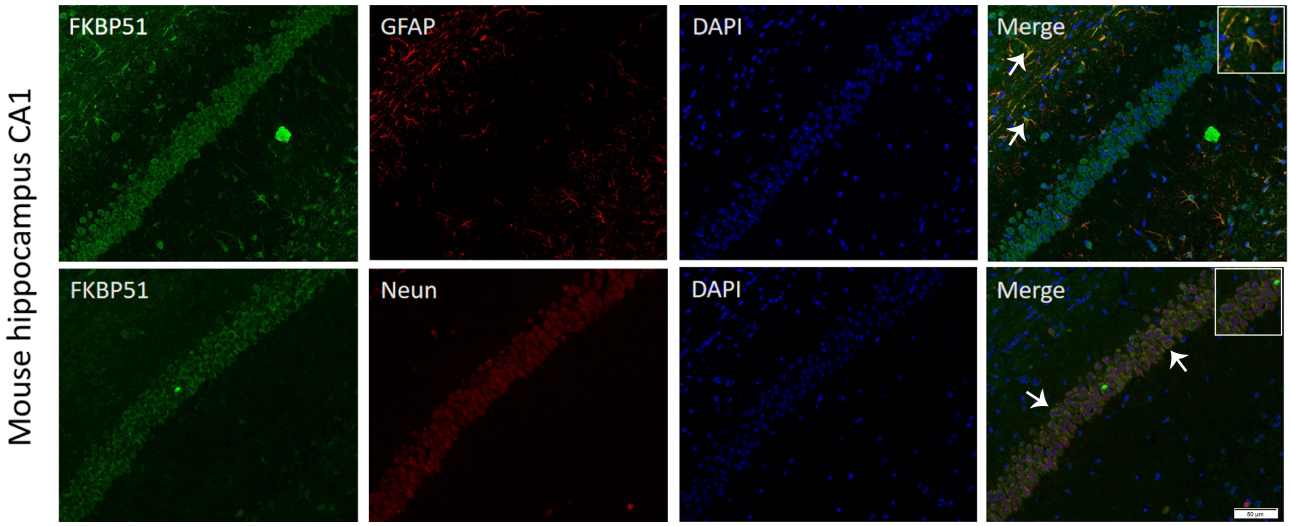

Fig. 2. Localization of FKBP51 in epileptic brain tissue detected by immunofluorescence FKBP51 was expressed in the CA1 in the hippocampus of epileptic mice. White arrows indicate co-expression with GFAP and NeuN (n = 5). The scale bar represents 50 μm. GFAP, Glial fibrillary acidic protein; DAPI, 4′,6-diamidino-2-phenylindole.

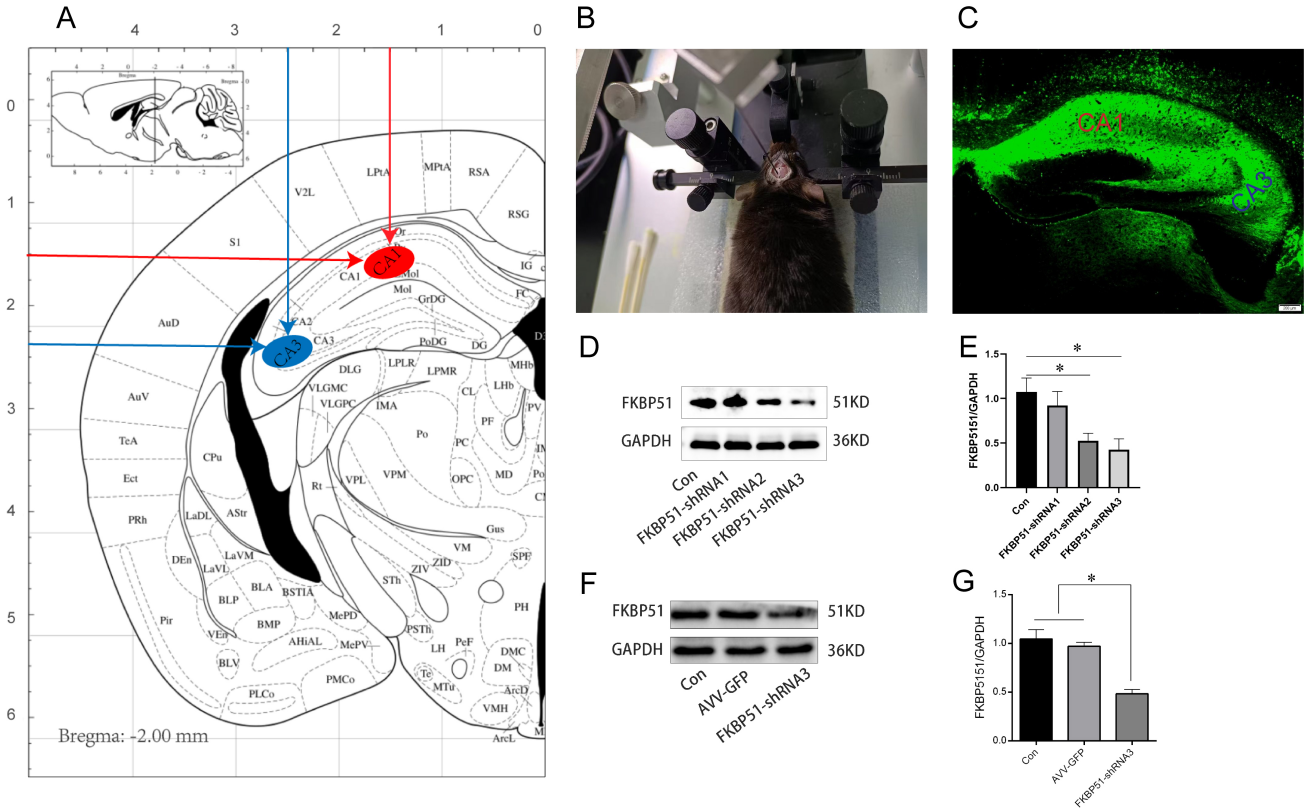

Fig. 3. Injection site and the selection of AAV-FKBP51-shRNA sequences. (A) According to the mouse atlas, the injection site is bilaterally symmetrical. (B) The AAV-FKBP51-shRNA stereotaxic injection procedure. (C) The fluorescence map of lentivirus transfection 4 weeks after injection of AAV-FKBP51-shRNA into hippocampal CA1 and CA3 of mice. The scale bar = 200 μm. (D,E) Three AAV-FKBP51-shRNA sequences infection efficiency in normal mice after 4 weeks of AAV-FKBP51-shRNA transfection (n = 5, ANOVAs: $F = 21.663$, $p = 0.0039 < 0.01$; Bonferroni post-hoc test, *α' < 0.0083 vs. Con group). (F,G) Expression of FKBP51 in hippocampal tissues of mice transfected with Gon, AVV-GFP and AAV-FKBP51-shRNA3 (n = 5, ANOVAs: $F = 65.329$, $p = 0.0085 < 0.01$; Bonferroni post-hoc test, *α' < 0.0167 vs. AAV-FKBP51-shRNA3 group). AAV-FKBP51-shRNA, adeno-associated virus-FK506-binding protein 51-small hairpin RNAs; GFP, green fluorescent protein.

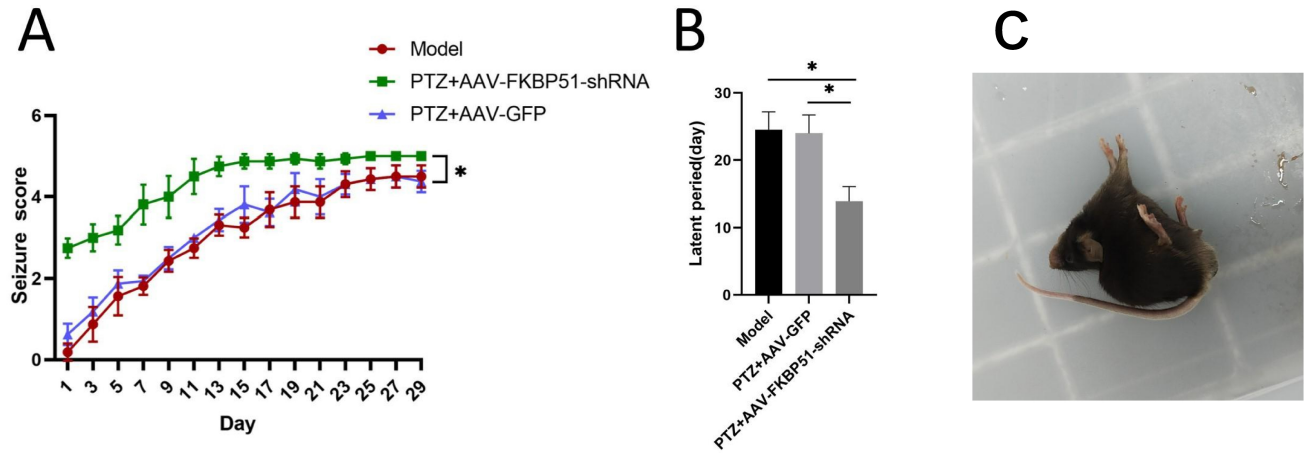

Fig. 4. Effects of FKBP51 on seizure grade and seizure latency in mice. (A,B) The seizure grades and latent period in the PTZ+AAV-FKBP51-shRNA group were significantly decreased compared to those in the Model group and PTZ+AAV-GFP group (n = 20, ANOVAs: F = 17.490, $p = 0.007 < 0.01$, Bonferroni post-hoc test, *α' < 0.0167 vs. AAV-FKBP51-shRNA group); (C) Images of grade 4 and 5 seizures in mice.

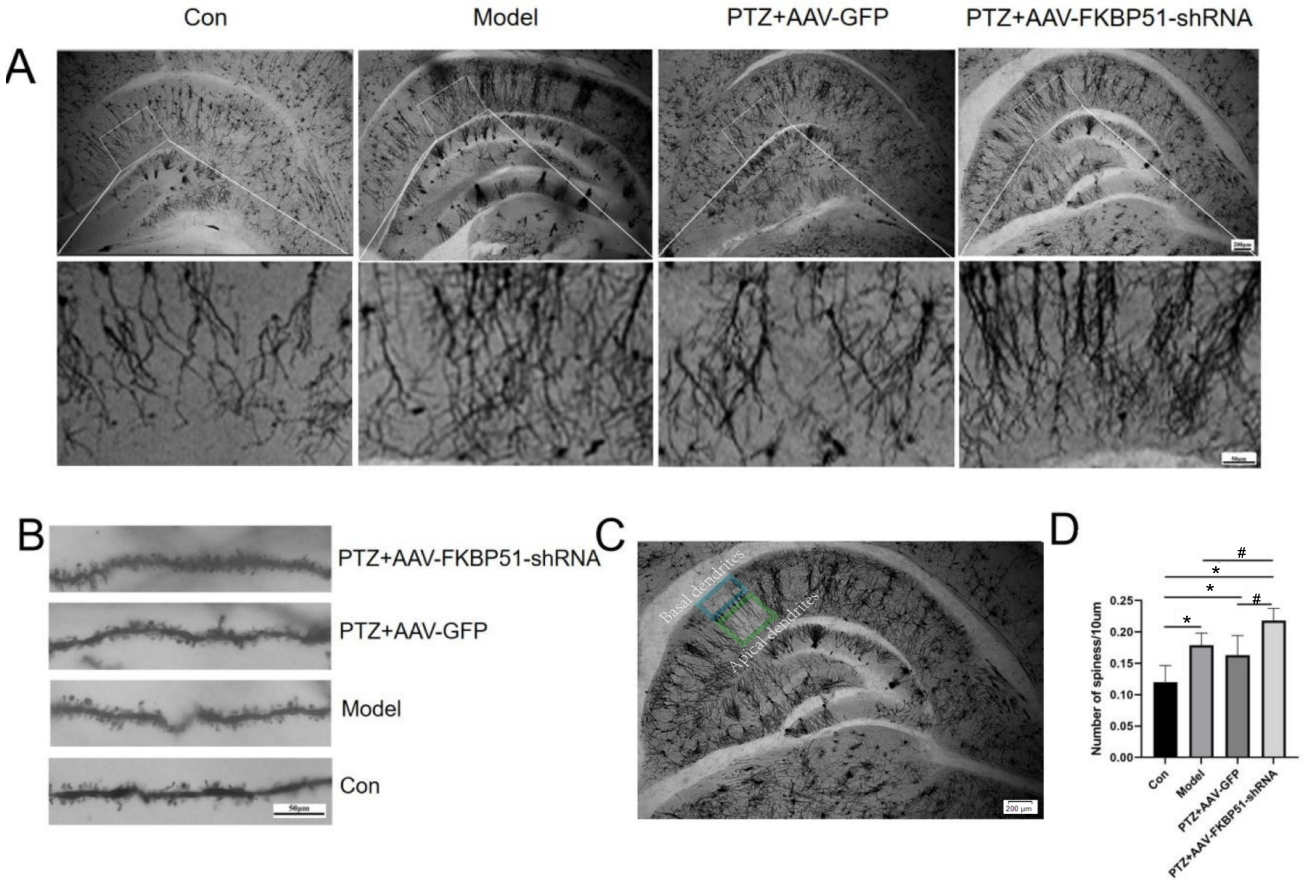

Fig. 5. Effect of endogenous FKBP51 inhibition on apical dendritic spines in CA1 of the hippocampus. (A) The distribution of apical dendritic spines in the hippocampal CA1 and local enlarged images of the Con group, Model group, PTZ+AAV-GFP group, and PTZ+AAV-FKBP51-shRNA group are shown. The scale bar = 200 μm, Upper; The scale bar = 50 μm, lower part. (B) The apical dendrites of the CA1 of the hippocampus in the Con group, Model group, PTZ+AAV-GFP group, and PTZ+AAV-FKBP51-shRNA group under oil microscope. The scale bar = 50 μm. (C) The top dendrites and bottom dendrites in CA1 (selected from the Model group). The scale bar = 200 μm. (D) The statistical histogram of apical dendritic spine density in the hippocampal CA1 of each group (n = 5, ANOVAs: F = 8.498, $p = 0.007 < 0.01$, Bonferroni post-hoc test, *α' < 0.0083 vs. Con group, #α' < 0.0083 vs. PTZ+AAV-FKBP51-shRNA group).

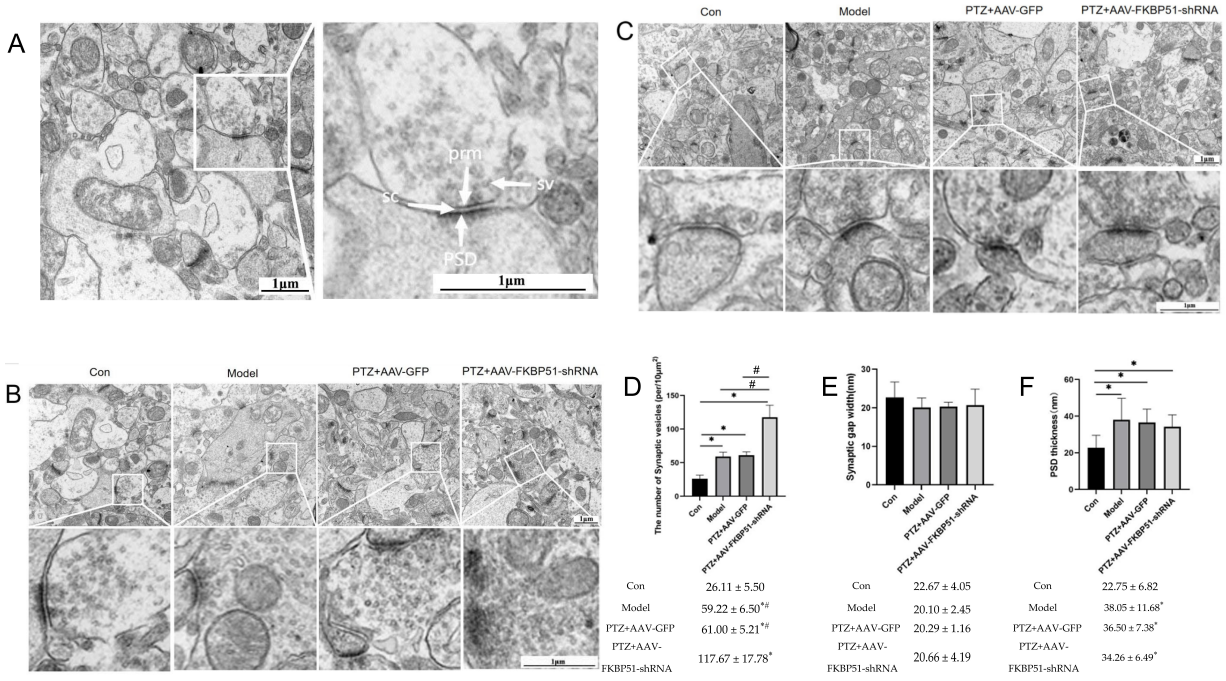

Fig. 6. Effect of endogenous FKBP51 inhibition on synaptic ultrastructure. (A) Clear synaptic structure (selected from Con group), presynaptic membrane (prm), synaptic cleft (sc), synaptic vesicles (sv), postsynaptic density (PSD), and other structures visible in the synaptic structure of the CA1 of the mouse hippocampus. The scale bar = 1 μm. (B) Representation of spherical synaptic vesicles in the presynaptic membrane of the Con group, Model group, PTZ+AAV-GFP group, and PTZ+AAV-FKBP51-shRNA group. The scale bar = 1 μm. (C) Representation of synaptic gap and postsynaptic density in Con group, Model group, PTZ+AAV-GFP group, and PTZ+AAV-FKBP51-shRNA group. The scale bar = 1 μm. (D–F) Statistical histograms of spherical synaptic vesicles, synaptic gap, and PSD95 thickness in the presynaptic membrane of each group, respectively (n = 5, Synaptic Vesicles: ANOVAs: $F = 53.076$, $p = 0.00013 < 0.01$, Synaptic Gap: ANOVAs: $F = 0.347$, $p = 0.347 > 0.05$, PSD95 thickness: ANOVAs: $F = 5.310$, $p = 0.026 < 0.05$, Bonferroni post-hoc test, Synaptic Vesicles: *α' < 0.0083 vs. Con group, #α' < 0.0083 vs. PTZ+AAV-FKBP51-shRNA group, PSD95 thickness: *α' < 0.0083 vs. Con group).

AAV-FKBP51-shRNA2 sequence inhibited approximately 44.0% expression of FKBP51 protein (α' < 0.0083). The AAV-FKBP51-shRNA3 sequence inhibited approximately 53.5% expression of the FKBP51 protein (α' < 0.0083, Fig. 3D,E). Thus, the AAV-FKBP51-shRNA3 sequence with the highest inhibitory efficiency was used for all experiments. Moreover, after injection of the AAV-FKBP51-shRNA3, the expression of FKBP51 was significantly decreased compared to the Con group and AVV-GFP group (α' < 0.0167, Fig. 3F,G). (n = 5, the original figures of western blot can be found in the **Supplementary Fig. 3**).

3.4 Effects of FKBP51 on Seizure Score and Seizure Latency in Mice

Behavioral results demonstrated that after intraperitoneal injection of PTZ, the seizure grade score of mice in the PTZ+AAV-FKBP51-shRNA group was significantly increased and the seizure latency was shortened considerably compared to the model group and PTZ+AAV-GFP group (n = 20, α' < 0.0167, Fig. 4). These results indicate that inhibition of endogenous FKBP51 shortened seizure latency and increased the seizure grade score in mice.

3.5 Effects of FKBP51 on Dendritic Spines

Dendritic spines are functional units of excitatory synapses involved in synaptic transmission. We observed the apical dendritic spines in the CA1 of the hippocampus within each group using Golgi staining. The results were as follows. Compared to the Con group, apical dendritic spines increased significantly in the Model group, with a statistically significant difference (α' < 0.0083). Compared to the Model group and PTZ+AAV-GFP group, the dendritic spine density in the PTZ+AAV-FKBP51-shRNA group increased, with a statistically significant difference (α' < 0.0083) (n = 5, Fig. 5).

3.6 Effects of FKBP51 on Synaptic Ultrastructure

The ultrastructure of synapses in the CA1 of the hippocampal tissue of mice in each group was observed using transmission electron microscopy. Subsequently, synaptic parameters (number of spherical synaptic vesicles per 10 μm^2, PSD thickness, and synaptic gap width) were statistically analyzed. The results, which are illustrated in Fig. 6 (n = 5, scale: 1 μm, magnification: 10,000× times), revealed

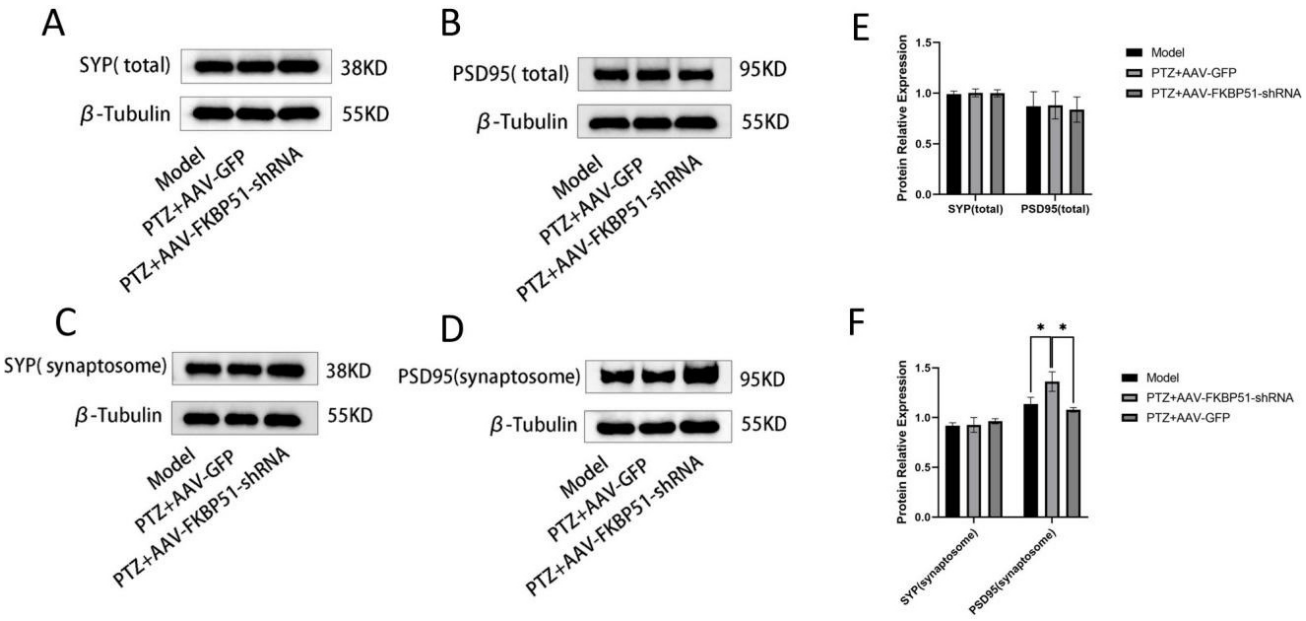

Fig. 7. Expression of PSD95 and SYP after decreasing the expression of FKBP51. (A–D) "Total PSD95 and SYP" and "PSD95 and SYP after extraction of synaptosomes" expression in the Model group, PTZ+AAV-GFP group, and PTZ+AAV-FKBP51-shRNA group after inhibition of endogenous FKBP51. (E) Statistical histogram of the expression of PSD95 and SYP before extracting the synaptosomes (n = 5, SYP: ANOVAs: F = 0.221, $p = 0.808 > 0.05$; PSD95: ANOVAs: F = 0.117, $p = 0.891 > 0.05$). (F) Statistical histogram of the expression of PSD95 and SYP after extracting the synaptosomes (n = 5, SYP: ANOVAs: F = 0.385, $p = 0.696 > 0.05$; PSD95: ANOVAs: F = 18.068, $p = 0.003 < 0.01$; Bonferroni post-hoc test, *α' < 0.0167 vs. AAV-FKBP51-shRNA group).

the following: (1) synaptic vesicles: a uniform distribution of spherical synaptic vesicles was observed in the CA1 of the hippocampus of mice in all groups. Compared to the Con group, the number of spherical synaptic vesicles per 10 μm^2 was significantly increased in the Model group ($\alpha' <$ 0.0083, Fig. 6D). Similarly, compared to the Model group and PTZ+AAV-GFP group, the number of spherical synaptic vesicles per 10 μm^2 in the PTZ+AAV-FKBP51-shRNA group was significantly increased ($\alpha' < 0.0083$, Fig. 6D). (2) PSD thickness: PSD thickness was significantly increased in the model group compared to the Con group ($\alpha' < 0.0083$, Fig. 6F). There was no significant difference in PSD thickness among the model group, PTZ+AAV-GFP group, and PTZ+AAV-FKBP51-shRNA group ($\alpha' > 0.0083$, Fig. 6F). (3) Synaptic gap width: between the groups, there were no significant differences ($\alpha' > 0.0083$, Fig. 6E) (n = 5, Fig. 6).

3.7 Expression of PSD95 and SYP in Hippocampal Tissues of Mice in Each Group after 4 Weeks of Successful Transfection with Adeno-Associated Virus

A mouse model of epilepsy was induced by intraperitoneal PTZ injection 4 weeks after stereoscopic AAV-FKBP51-shRNA injection into the CA1 of the bilateral hippocampus. After successful modeling, bilateral hippocampal tissues of each group of mice were analyzed using western blotting. The results revealed that after endogenous FKBP51 inhibition, there were no significant differences in PSD95 and SYP protein expression in the model group, PTZ+AAV-GFP group, or PTZ+AAV-FKBP51-shRNA group ($\alpha' > 0.0167$, Fig. 7A,B,E). After extraction of synaptosomes from the hippocampus, PSD95 protein expression in the PTZ+AAV-FKBP51-shRNA group was significantly higher than that in the model group and PTZ+AAV-GFP group ($\alpha' < 0.0167$, Fig. 7D,F), whereas SYP expression was not significantly different ($\alpha' > 0.0167$, Fig. 7C,F). (n = 5, Fig. 7 and the original figures of western blot can be found in the **Supplementary Fig. 4**).

4. Discussion

The pathophysiology of epilepsy has been the subject of many studies in recent years, including signaling pathways, ion channels, receptors, proteins, and enzymes [42–44]. This study is the first to demonstrate the involvement of FKBP51 in the development of epilepsy. Our findings suggest that FKBP51 may regulate the expression of the synaptic plasticity-related protein PSD95, dendritic spine density, and the number of synaptic vesicles in the hippocampal CA1 region, thereby functioning as an endogenous protective factor in epilepsy development. Our study assessed FKBP51 protein expression in the hippocampus of PTZ- and KA-induced epileptic mice. The results revealed that the expression of FKBP51 protein increased in both the PTZ-induced epileptic model and the KA-induced epileptic model. No significant differences were observed

in the total expression of PSD95 and SYP proteins. However, in the hippocampal synaptosomes in the Model group, the expression of PSD95 and SYP decreased. Additionally, subcellular localization by immunofluorescence revealed that FKBP51 was mainly localized in the neuronal cell membrane and was partially expressed in astrocytes. A study has demonstrated that astrocytes are involved in epilepsy development in various ways [45]. Araque *et al*. [46] reported that astrocytes not only provide support and nutrition to neurons but also participate in the modulation of synaptic transmission and synaptic plasticity. Furthermore, astrocytes are involved in the modulation and release of neurotransmitters associated with epileptic seizures, enhancing synaptic transmission and neuronal excitability, which contributes to the development of epilepsy [47,48]. Based on these results, we used AAV-FKBP51-shRNA to inhibit endogenous FKBP51 protein expression. We found that inhibiting endogenous FKBP51 significantly shortened seizure latency and increased seizure scores. These results indicate that FKBP51 is involved in seizure occurrence as an endogenous protective factor.

After establishing a correlation between FKBP51 and epilepsy, we further investigated the effects of FKBP51 on the synaptic plasticity of hippocampal neurons in mice. Previous researchers have identified dendritic spines as the postsynaptic sites of most excitatory glutamatergic synapses [49,50]. Neuronal dendritic branches and spines integrate most excitatory synaptic inputs required for normal synaptic transmission in the mammalian cortex and hippocampus, directly affecting the excitability of neurons and leading to epileptic seizures [51]. A previous study found that increased dendritic spine density increases neuronal excitability [52]. However, decreased dendritic spine density decreases seizure duration and scores [53,54]. In addition, it was recently suggested that changes in dendritic spine morphology or numbers can disrupt the balance between excitation and inhibition in the brain, leading to epileptic seizures [51]. Our study found that inhibiting endogenous FKBP51 increased the density of dendritic spines, indicating that FKBP51 increased susceptibility to seizures by increasing dendritic spine density. However, current research results regarding the effects of FKBP51 on neuronal excitability are inconsistent. Most studies demonstrated that inhibiting the expression of FKBP51 promotes dendrites and dendritic spine growth, thereby increasing neuronal excitability [23–25,55]. Conversely, another study indicated that FKBP5 knockout reduces neuronal excitability [26]. Our findings align with most studies, as we observed increased dendritic spine density after inhibiting endogenous FKBP51.

Synapses, introduced in 1897, are asymmetric intercellular junctions that mediate rapid point-to-point communication between neurons or between neurons and muscles or glands [56,57]. Chemical or electrical junctions are the two main types of communication. Since they release neurotransmitters, most synapses are considered chemical in the CNS and spinal cord [57]. Chemical synapses are mainly categorized into two types (Type I and Type II) [58]. Type I synapses (asymmetric synapses) have a higher postsynaptic density than presynaptic vesicles, and their synaptic vesicles are spherical or round. These synapses are generally considered to be excitatory and are mainly distributed on dendritic spines, shafts, and cell bodies. In Type II synapses (symmetric synapses), the pre- and postsynaptic membranes have less dense substances, and their synaptic vesicles are flat or pleomorphic. These synapses are generally considered inhibitory and are mainly distributed on dendritic shafts and cell bodies [58]. Synapses are the basic elements of neural circuits and networks that communicate all aspects of brain function [59]. Many neuropsychiatric diseases are thought to be caused by pathological changes in synaptic structure and function, such as autism spectrum disorder, schizophrenia, obsessive-compulsive disorder, depression, Alzheimer's disease, and epilepsy [60–64]. A study has indicated that the remodeling of neuronal synaptic structures is involved in epilepsy occurrence [65]. Abnormal synaptic connections between neurons gradually enhance neuronal excitability, thereby increasing the susceptibility to spontaneous seizures in epilepsy [7,8]. In this study, we observed spherical or round synaptic vesicles in the presynaptic membrane of the mice hippocampus. Compared to the Con group, the number of spherical synaptic vesicles in the presynaptic membrane of the CA1 area increased in the model group. Furthermore, the number of spherical synaptic vesicles in the PTZ+AAV-FKBP51-shRNA group was further increased compared to that in the model and PTZ+AAV-GFP groups.

Synaptic plasticity is mainly manifested by changes in the synaptic morphology and density, and the formation of new synapses. A previous study has indicated that appropriately narrowing the synaptic gap can increase the concentration of neurotransmitters in the synaptic gap, enhance receptor activation in postsynaptic structures, and improve synaptic information transmission [66]. Our study only found that after inhibiting endogenous FKBP51, the density of dendritic spines increased, which is consistent with the results of Matosin *et al*. [22]. However, there were no significant differences in synaptic gaps between the groups, which suggested that synaptic gap is not directly responsible for the excitability of neurons, but it plays a crucial role in the process of neurotransmitter transmission. Finally, the effects of endogenous FKBP51 inhibition on synaptic plasticity-related proteins were examined. The PSD is an electron-dense region attached to the postsynaptic membrane, critical for synaptic strength and plasticity in excitatory neurons [67]. Numerous studies have demonstrated that dysregulation of PSD underlies many CNS diseases, such as depression, schizophrenia, autism spectrum disorder, and neurodegenerative diseases [68–71]. These include the PSD95, NMDA receptors, AMPA receptors, calcium/calmodulin-dependent protein kinase II, and actin

[67]. PSD95, a major synaptic protein, is crucial in excitatory synaptic transmission and postsynaptic density [72]. It is essential for the plasticity of excitatory neurons, and overexpression of PSD95 increases synaptic transmission [73]. This study found that after inhibiting endogenous FKBP51, PSD95 expression increased, indicating increased synaptic transmission. However, there was no significant change in PSD thickness, possibly because the occurrence of epilepsy had already significantly increased PSD thickness. Based on this, the influence of FKBP51 on PSD thickness was not obvious. It is also possible that the increased amount of PSD95 synthesis was insufficient to cause a change in PSD thickness.

A recent study has found that after FKBP5 knockout, LTP, the frequency of mEPSC in the hippocampus, and the expression of excitatory glutamate receptors are reduced [26]. However, the correlation with epilepsy has not been confirmed. The mechanisms underlying the association between FKBP51 and epilepsy need to be further explored.

5. Conclusions

Our study found that the expression of FKBP51 was increased and the expression of SYP and PSD95 was decreased in epileptic mice. After inhibiting endogenous FKBP51, the latency period shortened, and the severity of seizures in mice increased. And after inhibition of FKBP51 in the mice's hippocampus, PSD95 protein expression was significantly increased, whereas SYP expression was not changed. These findings indicate that FKBP51 may be involved in the occurrence of epilepsy as an endogenous protective factor by regulating the expression of PSD95, hippocampus CA1 region spine density, and number of synaptic vesicles. Consequently, FKBP51 may serve as a novel target for epilepsy treatment.

6. Limitations

The primary constraint of this study is the limited sample size, which might have introduced statistical biases and affected the generalizability of our results. The small number of mice might have increased variability and the risk of Type I and Type II errors. Future studies with larger cohorts are warranted to validate our findings and to further explore the relationship between FKBP51, synaptic plasticity, and susceptibility to epilepsy. Despite these limitations, our results provide a foundation for further investigation into the molecular mechanisms underlying epilepsy. Additionally, future research should include experiments to investigate the role of FKBP51 within astrocytes and its potential impact on epilepsy outcomes. Finally, the whole-cell patch clamp technique should be incorporated in future studies to examine the electrophysiological mechanisms of FKBP51 in epileptogenesis.

Availability of Data and Materials

Data will be made available from the corresponding author on request.

Author Contributions

HH and ZX conceptualized and designed the study, and LC wrote this paper. LC, WC, JQ, MZ, HZ, and JY contributed to the experiments and data analysis. All authors contributed to editorial changes in the manuscript. All authors read and approved the final manuscript. All authors have participated sufficiently in the work and agreed to be accountable for all aspects of the work.

Ethics Approval and Consent to Participate

All animal experiments adhered to the Guide for the Care and Use of Laboratory Animals (NIH Publication No. 80-23) and accordance with the Animal Ethics Committee of the Affiliated Hospital of Zunyi Medical University and were approved by the same committee (KLL(A)-2021-02).

Acknowledgment

The authors are grateful to Dr. Yi Zhou for providing academic advice.

Funding

This paper was supported by grants from the National Natural Science Foundation of China (Nos. 81760247, 82171450, 32160190).

Conflict of Interest

The authors declare no conflict of interest.

Supplementary Material

Supplementary material associated with this article can be found, in the online version, at https://doi.org/10.31083/JIN25710.

References

[1] Abokrysha NT, Taha N, Shamloul R, Elsayed S, Osama W, Hatem G. Clinical, radiological and electrophysiological predictors for drug-resistant epilepsy. The Egyptian Journal of Neurology, Psychiatry and Neurosurgery. 2023; 59: 44. https://doi.org/10.1186/s41983-023-00647-1.

[2] Shevlyakov AD, Kolesnikova TO, de Abreu MS, Petersen EV, Yenkoyan KB, Demin KA, *et al*. Forward Genetics-Based Approaches to Understanding the Systems Biology and Molecular Mechanisms of Epilepsy. International Journal of Molecular Sciences. 2023; 24: 5280. https://doi.org/10.3390/ijms24065280.

[3] Hu T, Zhang J, Wang J, Sha L, Xia Y, Ortyl TC, *et al*. Advances in Epilepsy: Mechanisms, Clinical Trials, and Drug Ther-apies. Journal of Medicinal Chemistry. 2023; 66: 4434–4467. https://doi.org/10.1021/acs.jmedchem.2c01975.

[4] Engel T. The P2X7 Receptor as a Mechanistic Biomarker for Epilepsy. International Journal of Molecular Sciences. 2023; 24: 5410. https://doi.org/10.3390/ijms24065410.

[5] de Bartolomeis A, Barone A, Buonaguro EF, Tomasetti C, Vellucci L, Iasevoli F. The Homer1 family of proteins at the crossroad of dopamine-glutamate signaling: An emerging molecular "Lego" in the pathophysiology of psychiatric disorders. A systematic review and translational insight. Neuroscience and Biobehavioral Reviews. 2022; 136: 104596. https://doi.org/10.1016/j.neubiorev.2022.104596.

[6] Cachope R, Pereda AE. Regulatory Roles of Metabotropic Glutamate Receptors on Synaptic Communication Mediated by Gap Junctions. Neuroscience. 2021; 456: 85–94. https://doi.org/10.1016/j.neuroscience.2020.06.034.

[7] Da Silva FHL, Gorter JA, Wadman WJ. Epilepsy as a dynamic disease of neuronal networks. Handbook of Clinical Neurology. 2012; 107: 35–62. https://doi.org/10.1016/B978-0-444-52898-8.00003-3.

[8] Faingold CL, Blumenfeld H. Targeting Neuronal Networks with Combined Drug and Stimulation Paradigms Guided by Neuroim-aging to Treat Brain Disorders. The Neuroscientist: a Review Journal Bringing Neurobiology, Neurology and Psychiatry. 2015; 21: 460–474. https://doi.org/10.1177/1073858415592377.

[9] Südhof TC. Towards an Understanding of Synapse Formation. Neuron. 2018; 100: 276–293. https://doi.org/10.1016/j.neuron.2018.09.040.

[10] Kamat PK, Kalani A, Rai S, Swarnkar S, Tota S, Nath C, *et al*. Mechanism of Oxidative Stress and Synapse Dysfunction in the Pathogenesis of Alzheimer's Disease: Understanding the Therapeutics Strategies. Molecular Neurobiology. 2016; 53: 648–661. https://doi.org/10.1007/s12035-014-9053-6.

[11] Luo L. Architectures of neuronal circuits. Science (New York, N.Y.). 2021; 373: eabg7285. https://doi.org/10.1126/science.abg7285.

[12] Stampanoni Bassi M, Iezzi E, Gilio L, Centonze D, Buttari F. Synaptic Plasticity Shapes Brain Connectivity: Implications for Network Topology. International Journal of Molecular Sciences. 2019; 20: 6193. https://doi.org/10.3390/ijms20246193.

[13] Qiao H, Li MX, Xu C, Chen HB, An SC, Ma XM. Dendritic Spines in Depression: What We Learned from Animal Models. Neural Plasticity. 2016; 2016: 8056370. https://doi.org/10.1155/2016/8056370.

[14] Li Q, Li QQ, Jia JN, Liu ZQ, Zhou HH, Mao XY. Targeting gap junction in epilepsy: Perspectives and challenges. Biomedicine & Pharmacotherapy = Biomedecine & Pharmacotherapie. 2019; 109: 57–65. https://doi.org/10.1016/j.biopha.2018.10.068.

[15] Bailus BJ, Scheeler SM, Simons J, Sanchez MA, Tshilenge KT, Creus-Muncunill J, *et al*. Modulating FKBP5/FKBP51 and autophagy lowers HTT (huntingtin) levels. Autophagy. 2021; 17: 4119–4140. https://doi.org/10.1080/15548627.2021.1904489.

[16] Agam G, Atawna B, Damri O, Azab AN. The Role of FKBPs in Complex Disorders: Neuropsychiatric Diseases, Cancer, and Type 2 Diabetes Mellitus. Cells. 2024; 13: 801. https://doi.org/10.3390/cells13100801.

[17] Pelleymounter LL, Moon I, Johnson JA, Laederach A, Halvorsen M, Eckloff B, *et al*. A novel application of pattern recognition for accurate SNP and indel discovery from high-throughput data: targeted resequencing of the glucocorticoid receptor co-chaperone FKBP5 in a Caucasian population. Molecular Genetics and Metabolism. 2011; 104: 457–469. https://doi.org/10.1016/j.ymgme.2011.08.019.

[18] Criado-Marrero M, Rein T, Binder EB, Porter JT, Koren J, 3rd, Blair LJ. Hsp90 and FKBP51: complex regulators of psychiatric diseases. Philosophical Transactions of the Royal Society of London. Series B, Biological Sciences. 2018; 373: 20160532. https://doi.org/10.1098/rstb.2016.0532.

[19] Gassen NC, Hartmann J, Zschocke J, Stepan J, Hafner K, Zellner A, *et al*. Association of FKBP51 with priming of au-tophagy pathways and mediation of antidepressant treatment response: evidence in cells, mice, and humans. PLoS Medicine. 2014; 11: e1001755. https://doi.org/10.1371/journal.pmed.1001755.

[20] Gassen NC, Hartmann J, Schmidt MV, Rein T. FKBP5/FKBP51 enhances autophagy to synergize with antidepressant action. Autophagy. 2015; 11: 578–580. https://doi.org/10.1080/15548627.2015.1017224.

[21] Blair LJ, Criado-Marrero M, Zheng D, Wang X, Kamath S, Nordhues BA, *et al*. The Disease-Associated Chaperone FKBP51 Impairs Cognitive Function by Accelerating AMPA Receptor Recycling. eNeuro. 2019; 6: ENEURO.0242–18.2019. https://doi.org/10.1523/ENEURO.0242-18.2019.

[22] Matosin N, Arloth J, Czamara D, Edmond KZ, Maitra M, Fröhlich AS, *et al*. Associations of psychiatric disease and ageing with FKBP5 expression converge on superficial layer neurons of the neocortex. Acta Neuropathologica. 2023; 145: 439–459. https://doi.org/10.1007/s00401-023-02541-9.

[23] Quintá HR, Maschi D, Gomez-Sanchez C, Piwien-Pilipuk G, Galigniana MD. Subcellular rearrangement of hsp90-binding im-munophilins accompanies neuronal differentiation and neurite outgrowth. Journal of Neurochemistry. 2010; 115: 716–734. https://doi.org/10.1111/j.1471-4159.2010.06970.x.

[24] Criado-Marrero M, Smith TM, Gould LA, Kim S, Penny HJ, Sun Z, *et al*. FKBP5 and early life stress affect the hippo-campus by an age-dependent mechanism. Brain, Behavior, & Immunity - Health. 2020; 9: 100143. https://doi.org/10.1016/j.bbih.2020.100143.

[25] Codagnone MG, Kara N, Ratsika A, Levone BR, van de Wouw M, Tan LA, *et al*. Inhibition of FKBP51 induces stress resilience and alters hippocampal neurogenesis. Molecular Psychiatry. 2022; 27: 4928–4938. https://doi.org/10.1038/s41380-022-01755-9.

[26] Qiu B, Xu Y, Wang J, Liu M, Dou L, Deng R, *et al*. Loss of FKBP5 Affects Neuron Synaptic Plasticity: An Electrophysiology Insight. Neuroscience. 2019; 402: 23–36. https://doi.org/10.1016/j.neuroscience.2019.01.021.

[27] Yang J, Zhang L, Cao LL, Qi J, Li P, Wang XP, *et al*. MicroRNA-99a is a Potential Target for Regulating Hypothalamic Synaptic Plasticity in the Peri/Postmenopausal Depression Model. Cells. 2019; 8: 1081. https://doi.org/10.3390/cells8091081.

[28] Bulovaite E, Qiu Z, Kratschke M, Zgraj A, Fricker DG, Tuck EJ, *et al*. A brain atlas of synapse protein lifetime across the mouse lifespan. Neuron. 2022; 110: 4057–4073.e8. https://doi.org/10.1016/j.neuron.2022.09.009.

[29] Bayés A, van de Lagemaat LN, Collins MO, Croning MDR, Whittle IR, Choudhary JS, *et al*. Characterization of the proteome, diseases and evolution of the human postsynaptic density. Nature Neuroscience. 2011; 14: 19–21. https://doi.org/10.1038/nn.2719.

[30] Levy AM, Gomez-Puertas P, Tümer Z. Neurodevelopmental Disorders Associated with PSD-95 and Its Interaction Partners. International Journal of Molecular Sciences. 2022; 23: 4390. https://doi.org/10.3390/ijms23084390.

[31] Fukata Y, Hirano Y, Miyazaki Y, Yokoi N, Fukata M. Transsynaptic LGI1-ADAM22-MAGUK in AMPA and NMDA recep-tor regulation. Neuropharmacology. 2021; 194: 108628. https://doi.org/10.1016/j.neuropharm.2021.108628.

[32] Lee Y, Zhang Y, Kim S, Han K. Excitatory and inhibitory synaptic dysfunction in mania: an emerging hypothesis from animal model studies. Experimental & Molecular Medicine. 2018; 50: 1–11. https://doi.org/10.1038/s12276-018-0028-y.

[33] Zhu ZA, Li YY, Xu J, Xue H, Feng X, Zhu YC, *et al*. CDKL5 deficiency in adult glutamatergic neurons alters synaptic activity and causes spontaneous seizures via TrkB signaling. Cell Reports. 2023; 42: 113202. https://doi.org/10.1016/j.celrep.2023.113202.

[34] Sarnat HB. Sequences of synaptogenesis in the human fetal and neonatal brain by synaptophysin immunocytochemistry. Frontiers in Cellular Neuroscience. 2023; 17: 1105183. https://doi.org/10.3389/fncel.2023.1105183.
[35] Jia C, Zhang R, Wei L, Xie J, Zhou S, Yin W, *et al*. Investigation of the mechanism of tanshinone IIA to improve cogni-tive function via synaptic plasticity in epileptic rats. Pharmaceutical Biology. 2023; 61: 100–110. https://doi.org/10.1080/13880209.2022.2157843.
[36] Sóki N, Richter Z, Karádi K, Lőrincz K, Horváth R, Gyimesi C, *et al*. Investigation of synapses in the cortical white matter in human temporal lobe epilepsy. Brain Research. 2022; 1779: 147787. https://doi.org/10.1016/j.brainres.2022.147787.
[37] Wang J, Yuan J, Pang J, Ma J, Han B, Geng Y, *et al*. Effects of Chronic Stress on Cognition in Male SAMP8 Mice. Cellular Physiology and Biochemistry: International Journal of Experimental Cellular Physiology, Biochemistry, and Pharmacology. 2016; 39: 1078–1086. https://doi.org/10.1159/000447816.
[38] Matosin N, Fernandez-Enright F, Lum JS, Engel M, Andrews JL, Gassen NC, *et al*. Molecular evidence of synaptic pa-thology in the CA1 region in schizophrenia. NPJ Schizophrenia. 2016; 2: 16022. https://doi.org/10.1038/npjschz.2016.22.
[39] Xin Y, Lin G, Hua T, Liang J, Sun T, Wu X. The altered expression of cytoskeletal and synaptic remodeling proteins during epi-lepsy. Open Life Sciences. 2023; 18: 20220595. https://doi.org/10.1515/biol-2022-0595.
[40] Becker A, Grecksch G, Schröder H. N omega-nitro-L-arginine methyl ester interferes with pentylenetetrazol-induced kindling and has no effect on changes in glutamate binding. Brain Research. 1995; 688: 230–232. https://doi.org/10.1016/0006-8993(95)00565-8.
[41] Shimada T, Yamagata K. Pentylenetetrazole-Induced Kindling Mouse Model. Journal of Visualized Experiments: JoVE. 2018; 56573. https://doi.org/10.3791/56573.
[42] Wei F, Yan LM, Su T, He N, Lin ZJ, Wang J, *et al*. Ion Channel Genes and Epilepsy: Functional Alteration, Pathogenic Potential, and Mechanism of Epilepsy. Neuroscience Bulletin. 2017; 33: 455–477. https://doi.org/10.1007/s12264-017-0134-1.
[43] Sanz P, Garcia-Gimeno MA. Reactive Glia Inflammatory Signaling Pathways and Epilepsy. International Journal of Molecular Sciences. 2020; 21: 4096. https://doi.org/10.3390/ijms21114096.
[44] Manford M. Recent advances in epilepsy. Journal of Neurology. 2017; 264: 1811–1824. https://doi.org/10.1007/s00415-017-8394-2.
[45] Vezzani A, Ravizza T, Bedner P, Aronica E, Steinhäuser C, Boison D. Astrocytes in the initiation and progression of epilepsy. Nature Reviews. Neurology. 2022; 18: 707–722. https://doi.org/10.1038/s41582-022-00727-5.
[46] Araque A, Parpura V, Sanzgiri RP, Haydon PG. Tripartite synapses: glia, the unacknowledged partner. Trends in Neurosciences. 1999; 22: 208–215. https://doi.org/10.1016/s0166-2236(98)01349-6.
[47] Devinsky O, Vezzani A, Najjar S, De Lanerolle NC, Rogawski MA. Glia and epilepsy: excitability and inflammation. Trends in Neurosciences. 2013; 36: 174–184. https://doi.org/10.1016/j.tins.2012.11.008.
[48] Verhoog QP, Holtman L, Aronica E, van Vliet EA. Astrocytes as Guardians of Neuronal Excitability: Mechanisms Underlying Epileptogenesis. Frontiers in Neurology. 2020; 11: 591690. https://doi.org/10.3389/fneur.2020.591690.
[49] Rossini L, De Santis D, Cecchini E, Cagnoli C, Maderna E, Cartelli D, *et al*. Dendritic spine loss in epileptogenic Type II focal cortical dysplasia: Role of enhanced classical complement pathway activation. Brain Pathology (Zurich, Switzerland). 2023; 33: e13141. https://doi.org/10.1111/bpa.13141.
[50] Rossini L, De Santis D, Mauceri RR, Tesoriero C, Bentivoglio M, Maderna E, *et al*. Dendritic pathology, spine loss and synaptic reorganization in human cortex from epilepsy patients. Brain: a Journal of Neurology. 2021; 144: 251–265. https://doi.org/10.1093/brain/awaa387.
[51] Wong M, Guo D. Dendritic spine pathology in epilepsy: cause or consequence? Neuroscience. 2013; 251: 141–150. https://doi.org/10.1016/j.neuroscience.2012.03.048.
[52] Mucha M, Skrzypiec AE, Schiavon E, Attwood BK, Kucerova E, Pawlak R. Lipocalin-2 controls neuronal excitability and anxiety by regulating dendritic spine formation and maturation. Proceedings of the National Academy of Sciences of the United States of America. 2011; 108: 18436–18441. https://doi.org/10.1073/pnas.1107936108.
[53] Chen L, Luo T, Cui W, Zhu M, Xu Z, Huang H. Kalirin is involved in epileptogenesis by modulating the activity of the Rac1 signaling pathway. Journal of Chemical Neuroanatomy. 2023; 131: 102289. https://doi.org/10.1016/j.jchemneu.2023.102289.
[54] Yang M, Lin P, Jing W, Guo H, Chen H, Chen Y, *et al*. Beclin1 Deficiency Suppresses Epileptic Seizures. Frontiers in Molecular Neuroscience. 2022; 15: 807671. https://doi.org/10.3389/fnmol.2022.807671.
[55] Caffino L, Giannotti G, Malpighi C, Racagni G, Fumagalli F. Short-term withdrawal from developmental exposure to cocaine activates the glucocorticoid receptor and alters spine dynamics. European Neuropsychopharmacology: the Journal of the European College of Neuropsychopharmacology. 2015; 25: 1832–1841. https://doi.org/10.1016/j.euroneuro.2015.05.002.
[56] Südhof TC. The cell biology of synapse formation. The Journal of Cell Biology. 2021; 220: e202103052. https://doi.org/10.1083/jcb.202103052.
[57] Rubio ME. Ultrastructural and molecular features of excitatory and glutamatergic synapses. The auditory nerve synapses. Vitamins and Hormones. 2020; 114: 23–51. https://doi.org/10.1016/bs.vh.2020.04.010.
[58] GRAY EG. Axo-somatic and axo-dendritic synapses of the cerebral cortex: an electron microscope study. Journal of Anatomy. 1959; 93: 420–433.
[59] Gentile JE, Carrizales MG, Koleske AJ. Control of Synapse Structure and Function by Actin and Its Regulators. Cells. 2022; 11: 603. https://doi.org/10.3390/cells11040603.
[60] Bai Y, Wang H, Li C. SAPAP Scaffold Proteins: From Synaptic Function to Neuropsychiatric Disorders. Cells. 2022; 11: 3815. https://doi.org/10.3390/cells11233815.
[61] Ren F, Guo R. Synaptic Microenvironment in Depressive Disorder: Insights from Synaptic Plasticity. Neuropsychiatric Disease and Treatment. 2021; 17: 157–165. https://doi.org/10.2147/NDT.S268012.
[62] Ren E, Curia G. Synaptic Reshaping and Neuronal Outcomes in the Temporal Lobe Epilepsy. International Journal of Molecular Sciences. 2021; 22: 3860. https://doi.org/10.3390/ijms22083860.
[63] Jung S, Park M. Shank postsynaptic scaffolding proteins in autism spectrum disorder: Mouse models and their dysfunctions in behaviors, synapses, and molecules. Pharmacological Research. 2022; 182: 106340. https://doi.org/10.1016/j.phrs.2022.106340.
[64] Bairamian D, Sha S, Rolhion N, Sokol H, Dorothée G, Lemere CA, *et al*. Microbiota in neuroinflammation and synaptic dysfunction: a focus on Alzheimer's disease. Molecular Neurodegeneration. 2022; 17: 19. https://doi.org/10.1186/s13024-022-00522-2.
[65] Jaworski T. Control of neuronal excitability by GSK-3beta: Epilepsy and beyond. Biochimica et Biophysica Acta. Molecular Cell Research. 2020; 1867: 118745. https://doi.org/10.1016/j.bbamcr.2020.118745.

[66] Savtchenko LP, Rusakov DA. The optimal height of the synaptic cleft. Proceedings of the National Academy of Sciences of the United States of America. 2007; 104: 1823–1828. https://doi.org/10.1073/pnas.0606636104.

[67] Levy NS, Umanah GKE, Rogers EJ, Jada R, Lache O, Levy AP. IQSEC2-Associated Intellectual Disability and Autism. International Journal of Molecular Sciences. 2019; 20: 3038. https://doi.org/10.3390/ijms20123038.

[68] Tomasetti C, Iasevoli F, Buonaguro EF, De Berardis D, Fornaro M, Fiengo ALC, *et al*. Treating the Synapse in Major Psychiatric Disorders: The Role of Postsynaptic Density Network in Dopamine-Glutamate Interplay and Psychopharmacologic Drugs Molecular Actions. International Journal of Molecular Sciences. 2017; 18: 135. https://doi.org/10.3390/ijms18010135.

[69] Wilkinson B, Coba MP. Molecular architecture of postsynaptic Interactomes. Cellular Signalling. 2020; 76: 109782. https://doi.org/10.1016/j.cellsig.2020.109782.

[70] Moraes BJ, Coelho P, Fão L, Ferreira IL, Rego AC. Modified Glutamatergic Postsynapse in Neurodegenerative Disorders. Neu-roscience. 2021; 454: 116–139. https://doi.org/10.1016/j.neuroscience.2019.12.002.

[71] Samojedny S, Czechowska E, Pańczyszyn-Trzewik P, Sowa-Kućma M. Postsynaptic Proteins at Excitatory Synapses in the Brain-Relationship with Depressive Disorders. International Journal of Molecular Sciences. 2022; 23: 11423. https://doi.org/10.3390/ijms231911423.

[72] Bustos FJ, Ampuero E, Jury N, Aguilar R, Falahi F, Toledo J, *et al*. Epigenetic editing of the Dlg4/PSD95 gene improves cognition in aged and Alzheimer's disease mice. Brain: a Journal of Neurology. 2017; 140: 3252–3268. https://doi.org/10.1093/brain/awx272.

[73] Vallejo D, Codocedo JF, Inestrosa NC. Posttranslational Modifications Regulate the Postsynaptic Localization of PSD-95. Molecular Neurobiology. 2017; 54: 1759–1776. https://doi.org/10.1007/s12035-016-9745-1.